Journal of Power Sources 244 (2013) 429–434

Contents lists available at SciVerse ScienceDirect

Journal of Power Sources

journal homepage: www.elsevier.com/locate/jpowsour

Fe phthalocyanine supported by graphene nanosheet as catalyst in Li–air battery with the hybrid electrolyte

Eunjoo Yoo, Haoshen Zhou*

Energy Technology Research Institute, National Institute of Advanced Industrial Science and Technology, Umezono 1-1-1, Central 2, Tsukuba, Ibaraki 305-8568, Japan

HIGHLIGHTS

- The FePc supported on various carbon was used as an air electrode for Li–air batteries.
- The FePc/carbon catalysts exhibited the high catalytic activity of ORR.
- The FePc/CNTs showed a good discharge performance and stable cycling performance.

ARTICLE INFO

Article history:
Received 1 October 2012
Received in revised form
26 November 2012
Accepted 29 November 2012
Available online 12 December 2012

Keywords:
Fe phthalocyanine
Graphene nanosheet
Carbon nanotube
Li–air battery
Elctrocatalytic activity
Cathode catalysts

ABSTRACT

Non noble metal catalysts of cathode electrode for Li–air battery with hybrid electrolyte were prepared by the combination between Fe phthalocyanine (FePc) and different kinds of carbon such as graphene nanosheet (GNS), multi-wall carbon nanotubes (MWCNTs) and acetylene black (AB). The oxygen reduction reaction (ORR) of these FePc supported on carbon catalysts in alkaline media was studied. The onset potential of ORR for FePc supported on carbon shows −0.01 V *vs.* Ag/AgCl, which is near that of 20 wt% Pt/CB. Furthermore, rotating disk electrode (RDE) measurements show that the ORR mechanism is 4-electron pathway for all FePc supported on carbon. It is considered that the combination between FePc and carbon materials leads to synergic effect of electrocatalytic activity toward ORR. Moreover, the electrochemical performance of Li–air batteries exhibit that the FePc/CNTs not only provided a good discharge performance, but also showed a much more stable cycling performance than those of FePc/GNS and FePc/AB. It is thus considered that the electrochemical performance of Li–air battery is dependent on the kind of carbon materials.

1. Introduction

The Li–air battery has attracted much more attention due to its extremely high theoretical specific energy density because the use of negative lithium metal provides a rather high voltage of 3 V [1–3]. Considering the operational voltages 2.9–3.1 V for system using non-aqueous electrolyte, the theoretical energy density based on Li electrode can be about 3600 W h kg^{-1}, which includes a cathodic reaction of $2Li^+ + O_2 + 2e^- \rightarrow Li_2O_2$ and an anodic reaction of $2Li + 2e^- \rightarrow 2Li^+$ [4]. 3600 W h kg^{-1} is based on the total mass of oxygen and lithium. The Li–air batteries' with aqueous electrolyte energy density will be a little lower than that of the Li–air batteries with non-aqueous electrolyte. However, the Li–air batteries with non-aqueous electrolyte have still some critical problems such as air electrode's clogging and organic liquid electrolyte's decomposition during the discharge process. These problems lead to a short life of non-aqueous Li–air battery.

Recently, the Li–air batteries with aqueous electrolyte represent an alternative approach to overcome these problems. Zhang et al. have reported that the Li/PEO 18 LiTFSI/LTAP/aqueous LiCl/Pt air cell showed a stable open-circuit voltage of 3.70 V at 60 °C for 2 months [5]. Our group also has developed a new type rechargeable Li–air battery based on a hybrid electrolyte with an aqueous electrolyte in the air electrode side [6,7].

Generally, the platinum (Pt), platinum-based catalysts and metal oxide such as Mn_2O_3, Fe_2O_3, CuO, supported by carbons, have been used as a cathode electrode for Li–air battery [6,8]. We have also reported that the Li–air battery based on Mn_2O_3 supported carbon as a cathode electrode with a hybrid electrolyte; it showed the longer discharge time and stability for the discharge process. However, there are some problems to overcome as regards the secondary battery, especially the poor cycle performance. Thus it is necessary to find the efficient and durable of cathode catalysts for

* Corresponding author. Tel.: +81 29 861 5648; fax: +81 29 861 5799.
E-mail address: hs.zhou@aist.go.jp (H. Zhou).

0378-7753/$ – see front matter © 2012 Elsevier B.V. All rights reserved.
http://dx.doi.org/10.1016/j.jpowsour.2012.11.132

oxygen reduction reaction (ORR) alternatives to Pt and metal oxide supported carbon.

Recently, studies have implied that the iron phthalocyanine (FePc) is promising catalyst for the ORR [9,10]. Though much effort has been made for developing ORR catalysts, there are some problems in using it as a cathode electrode. For examples, the poor electron conductivity of FePc made the electron transfer in the ORR process difficult. To solve the problem, the FePc was supported on the high surface carbon area substrate such as Vulcan XC-72 and carbon black [11]. However, the ORR stability still needed a further improvement. Dong et al. have reported that the FePc loaded on single-walled carbon nanotubes (SWCNTs) showed the good catalytic activity of ORR and stability [12]. Although the FePc loaded on SWCNTs exhibited the high catalytic activity, the price of SWCNTs is very expensive to use the substrate of catalysts. Thus, it is necessary to find a carbon substrate with good conductivity and low-cost to consider the promising electrocatalysts of energy device of future.

Here, we report the effect of carbon substrate for FePc supported on various carbon materials and study not only the ORR activity, but also electrochemical performance of Li–air battery with a hybrid electrolyte. The graphene nanosheet (GNS), multi-walled carbon nanotubes (MWCNTs) and acetylene black (AB) were used as a carbon substrate. It is expected that the FePc can be easily adsorbed on CNTs and GNS via non-covalent π–π interactions facilitating the electron transfer process and stabilizing the systems. Cyclic voltamperometry (CV) and rotating disk electrode (RDE) measurement were performed to explore the electrocatalytic activity toward the ORR. The electrocatalytic activity of FePc/carbon for Li–air battery base on the hybrid electrolyte with alkaline media was studied by examining their discharge and cycle performance.

2. Experimental

GNS were obtained using precursor graphite as a starting material through the chemical reduction of graphene oxide in solution [13]. The reduction of graphite oxide was carried out stirring with hydrazine hydrate at room temperature for 24 h, then washed with distilled water until neutral and dried at room temperature for 24 h to obtain the GNS. The MWCNTs were purchased from micro phase company, which were prepared by a catalytic decomposition method of hydrocarbons. The FePc supported on various carbon materials was prepared by the following procedure. The carbon materials (GNS, MWCNTs, and AB) of 200 mg were dispersed in the ethanol with ultrasonification for 30 min, and then add the solution which dispersed FePc of 100 mg in the ethanol. Consequently, the mixed solution was ultrasonicated for 1 h and stirred at 80 °C to evaporate the ethanol.

The oxygen reduction reaction (ORR) activity was tested by using rotating disk electrode (RDE) with a three-electrode grass

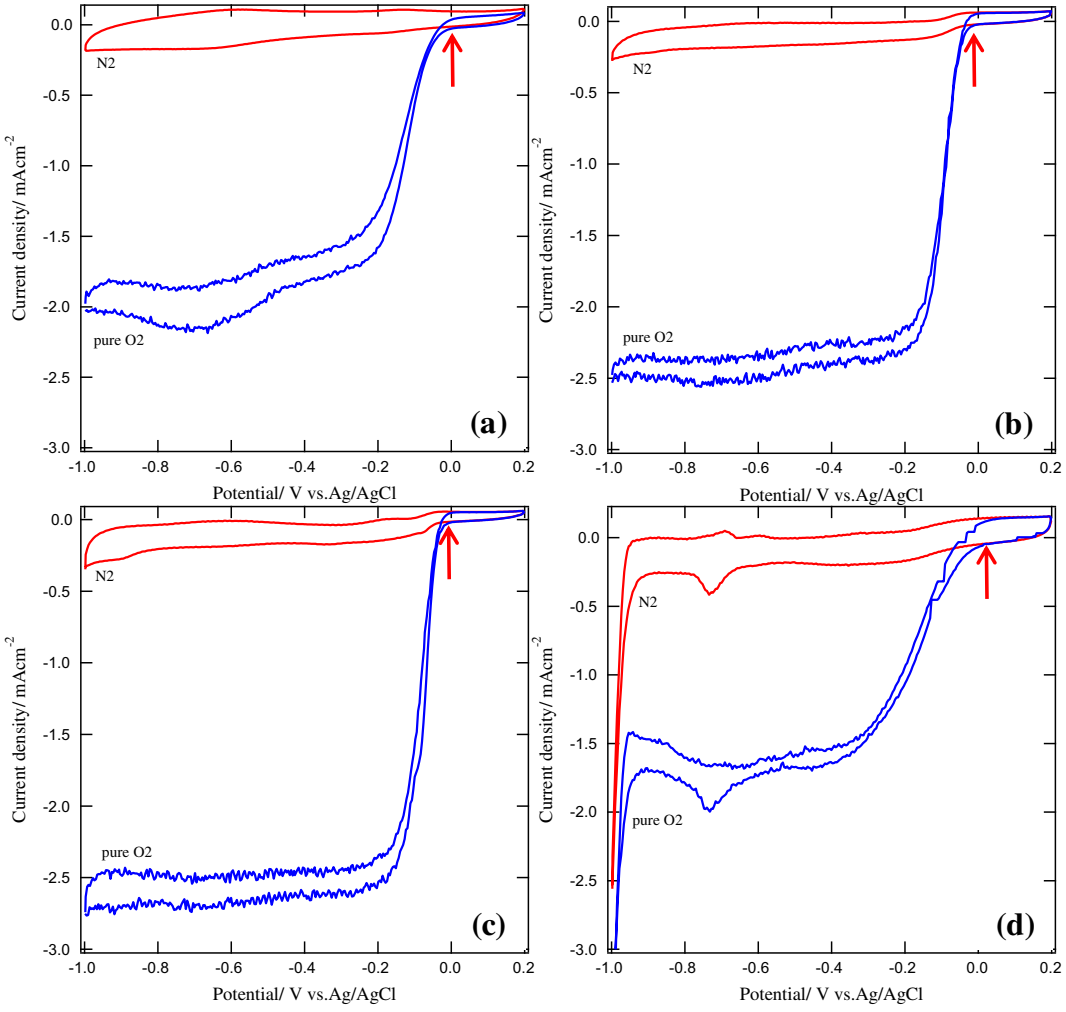

Fig. 1. CV curves of ORR for FePc/GNS (a), FePc/CNTs (b), FePc/AB (c) and 20 wt% Pt/CB (d) in alkaline media (1 M $LiNO_3$ + 0.5 M LiOH) at the scan rate of 20 mV s^{-1} with rotation rate of 500 rpm in nitrogen gas or pure oxygen gas.

cell, in the 1 M $LiNO_3$+0.5 M LiOH at room temperature, under a flow of nitrogen gas or pure oxygen gas. Catalysts were loaded onto a glassy carbon electrode (0.28 cm^2) with diluted (1:50 in methanol) 5 wt% Nafion solution (Aldrich). The working electrode was a catalyst supported on a glassy carbon disk, the counter electrode was a platinum and a silver/silver chloride electrode (Ag/AgCl) was used as the reference electrode.

The electrochemical test set up for Li–air battery with hybrid electrolyte was described in previous work of our group [6]. 1 M $LiClO_4$/ED/DEC was used as the organic electrolyte and 1 M $LiNO_3$+0.5 M LiOH was used as the aqueous electrolyte. Then, the solid state electrolyte $Li_{1+x+y}Al_x(Ti,Ge)_{2-x}Si_yP_{3-y}O_{12}$ (LISICON) film was used as the separating membrane between organic electrolyte and aqueous electrolyte to prevent intermixes between the two solutions. The catalysts paste was prepared by following procedure. The catalyst (FePc/GNS, FePc/AB and FePc/CNTs, respectively) (90%), polytetrafluoroethylene (PTFE) (7%) and AB (3%) were well mixed, and then was rolled-pressed into a sheet to form catalytic layer. The gas diffusion layer was prepared by mixing the AB (60%) and PTFE (40%), and then was rolled to form film. Consequently, the air catalytic layer was prepared by pressing the catalytic layer and gas diffusion layer onto nickel mesh. The cells were discharged at the current density of 0.5 mA cm^{-2} for 24 h in an ambient air condition. The charge–discharge performance was carried out in the voltage range from 2 to 4.8 V at the current density of 0.5 mA cm^{-2} for 2 h, respectively.

The FePc/GNS, FePc/AB and FePc/CNTs were characterized by scanning electron microscope (SEM) and Raman spectroscopy (Ventuno[21], JASCO, Tokyo). A commercial 20 wt% Pt/carbon black (CB) (Johnson Matthey) was also used as a reference at same investigation conditions to compare the ORR.

3. Result and discussion

Fig. 1 shows the cyclic voltammogram (CV) of ORR for FePc/GNS, FePc/CNTs, FePc/AB and 20 wt% Pt/CB at the scan rate of 20 mV s^{-1} with rotation rate of 500 rpm in nitrogen gas or pure oxygen gas. The onset potential of ORR for the FePc/GNS, FePc/CNTs and FePc/AB started at about −0.01 V *versus* Ag/AgCl. As expected, the onset potential of ORR for 20 wt% Pt/CB shows at 0.01 V *versus* Ag/AgCl. Furthermore, the current density at the overpotential of −0.1 V *versus* Ag/AgCl was −1.49, −0.64, −1.95 and −0.42 mA cm^{-2} for the FePc/CNTs, FePc/GNS, FePc/AB and 20 wt% Pt/CB, respectively. Interestingly, the FePc supported on various carbon materials show the high value of current density at −0.1 V *versus* Ag/AgCl, compared with 20 wt% Pt/CB, even though the onset potential of ORR was lower than that of 20 wt% Pt/CB. It is thus considered that the FePc supported on various carbon had much higher catalytic activity toward oxygen reduction.

Fig. 2(a–d) gives the linear sweep voltammogram (LSV) curves obtained for FePc/carbon and 20 wt% Pt/CB under the alkaline condition in the saturated pure O_2 at different rotation rate from 300 to 1500 rpm at the scan rate of 20 mV s^{-1} to investigate the number of electrons involved in the ORR as well as ORR mechanism. The polarization curves of FePc/carbon and 20 wt% Pt/CB display current plateaus in the high polarization range. The mass transport limiting ORR current for all measured samples was reached at −0.15 V. However, the ORR limiting currents for FePc/carbon were higher than those for the 20 wt% Pt/CB under the same rotation rate. The electrochemical reduction of O_2 is a multi-electron reaction that has two main possible pathways. One is the transfer of two electrons to produce H_2O_2 and the other is a direct four-electron pathway to produce water. In order to investigate further the ORR activity of FePc/carbon, the transferred electron number per oxygen molecules involved in the ORR process was analyzed by RDE to obtain the slope of Koutcky–Levich (K–L) plots. The Koutcky–Levich (K–L) equation was followed [14,15].

$$\frac{1}{j} = \frac{1}{j_k} + \frac{1}{B\omega^{\frac{1}{2}}}$$

where j represents the measured current density, j_k is the kinetic current density, and ω is the rotation rate of the electrode. B could

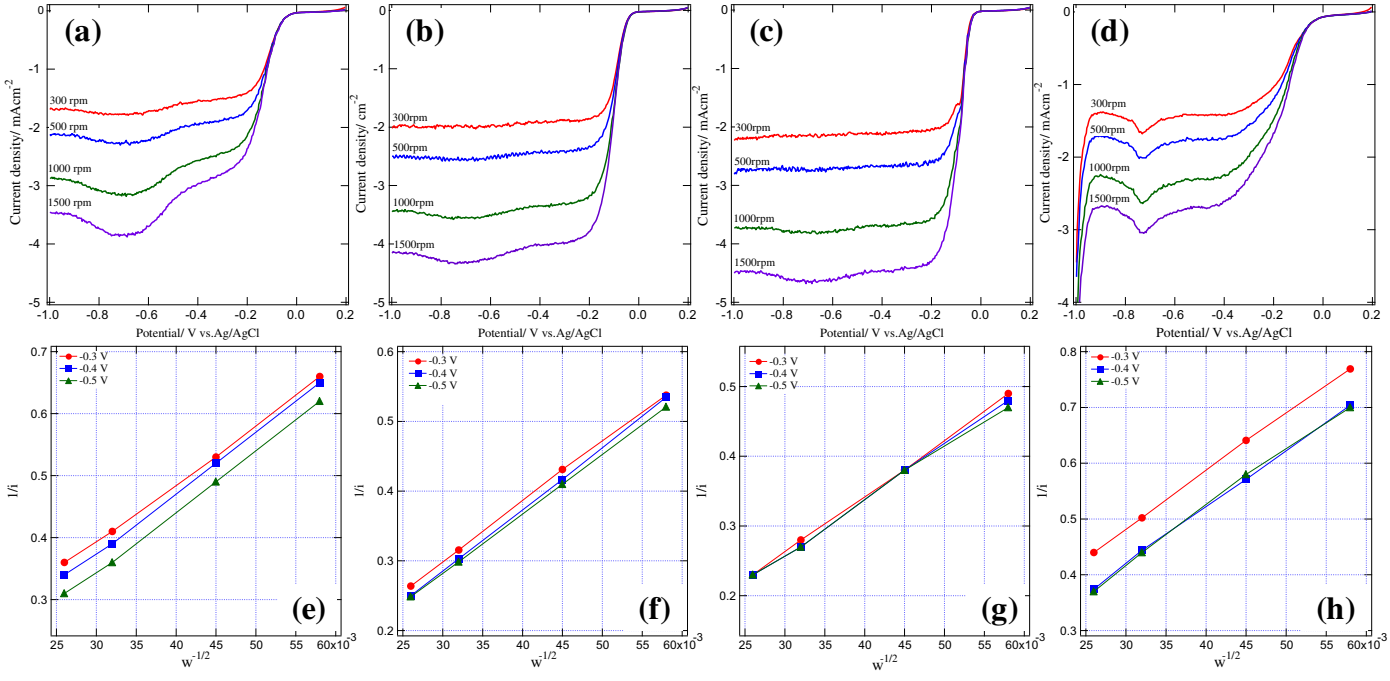

Fig. 2. Linear sweep voltammogram (LSV) curves for FePc/GNS (a), FePc/CNTs (b), FePc/AB (c) and 20 wt% Pt/CB (d) under the alkaline condition in the saturated pure O_2 at different rotation rate from 300 to 1500 rpm at the scan rate of 20 mV s^{-1}. Koutcky–Levich (K–L) plots of FePc/GNS (e), FePc/CNTs (f), FePc/AB (g) and 20 wt% Pt/CB (h) at fixed potential (−0.3, −0.4 and −0.5).

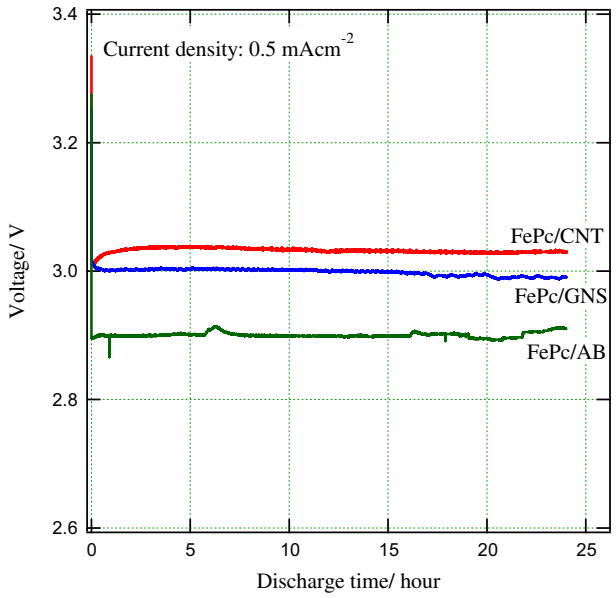

Fig. 3. Discharge curves of FePc supported on various carbon materials in alkaline condition (1 M $LiNO_3$ + 0.5 M LiOH) at current density of 0.5 mA cm^{-2} for 24 h.

be calculated from the slope of K–L plots based on the Levich equation as follows:

$$B = 0.2nF(D_{O_2})^{\frac{2}{3}}\nu^{\frac{1}{6}}C_{O_2}$$

where n is the number of electrons transferred, F is the Faraday constant ($F = 96485$ C mol^{-1}), D_{O_2} is the diffusion coefficient of O_2 gas, ν is the kinetic viscosity of 1.0 M $LiNO_3$ + 0.5 M LiOH solution, and C_{O_2} is the concentration of O_2 gas in dilute aqueous solution. Fig. 2(e–h) shows the Koutcky–Levich (K-L) plots of ($1/j$) *vs.* $\omega^{1/2}$ at a fixed potential (−0.3, −0.4 and −0.5) on the FePc/carbon and 20 wt% Pt/CB electrode derived from the data in Fig. 2(a–d). These Koutcky–Levich (K-L) plots show good linearity with parallelism suggesting a first-order dependence of O_2 kinetics on all electrodes. Moreover, it is well known that the oxygen reduction reaction by Pt/CB proceeds via a direct 4-electron pathway without the formation of H_2O_2 in an acidic or an alkaline media [16,17]. Therefore it is possible to gain a further understanding of the ORR pathway by FePc/carbon through comparative K–L plots. In this study, the number of electrons transferred for 20 wt% Pt/CB was assumed to 4-electron. According to the K–L equation, the number of electrons transferred for ORR in FePc/GNS, FePc/CNTs and FePc/AB was calculated to be about 4.1, 3.5, and 3.6, respectively. These results suggested that the ORR catalyzed on FePc/carbon is a close 4-electron reduction process leading to the formation of H_2O. It is thus indicated that the FePc played an important role for catalysts for ORR, because it is reported that the reaction of only carbon electrode is far less than four-electron reaction [18]. Based on the result, we also considered that the combination between FePc and carbon materials promoted the electrocatalytic activity for ORR.

The electrochemical performance of FePc/GNS, FePc/AB and FePc/CNTs was tested by using Li–air batteries with hybrid electrolyte. Fig. 3 gives the discharge curves of FePc/GNS, FePc/AB and FePc/CNTs at a current density of 0.5 mA cm^{-2} for 24 h. The discharge voltage was 3.03, 3.0 and 2.9 V for FePc/CNTs, FePc/GNS

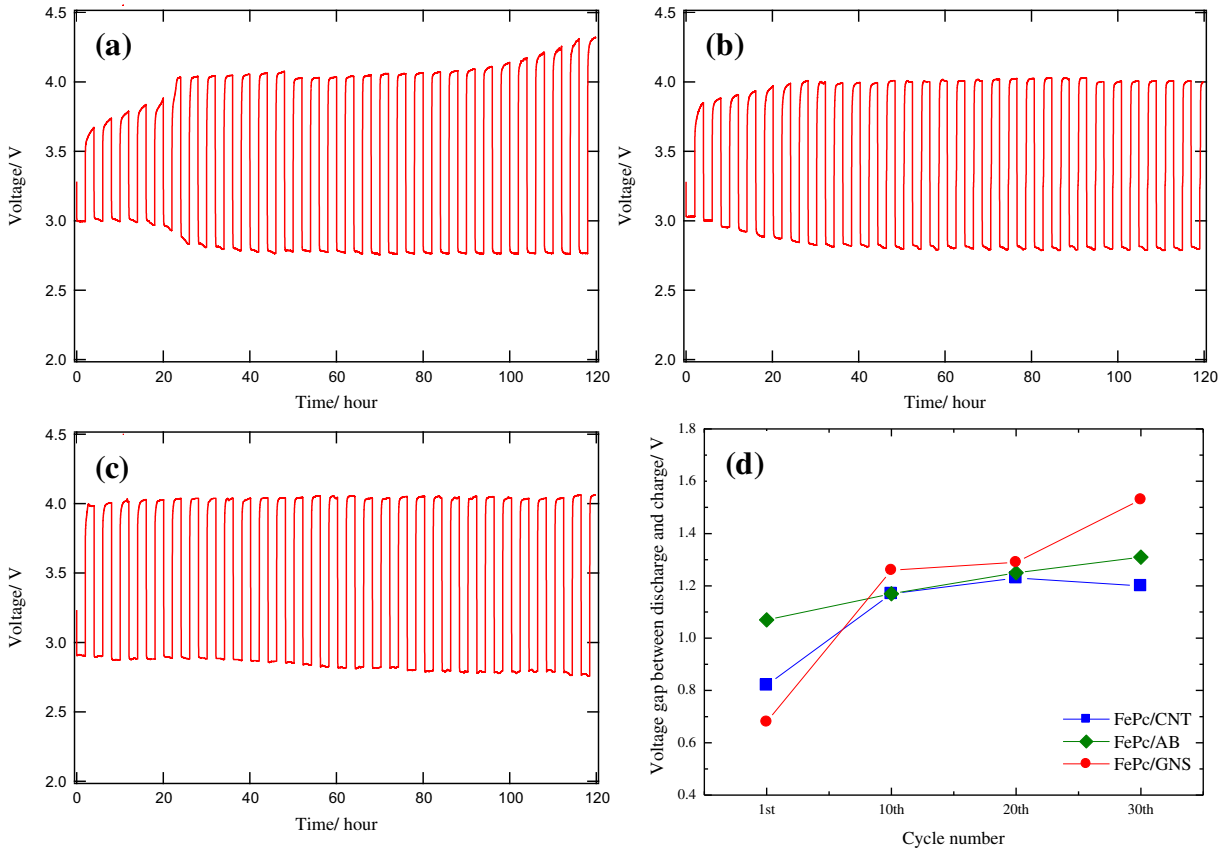

Fig. 4. Cyclic performances of FePc/GNS (a), FePc/CNTs (b), and FePc/AB (c) at current density of 0.5 mA cm^{-2} for 30th cycle. The voltage gap between discharge and charge for all measured samples (d).

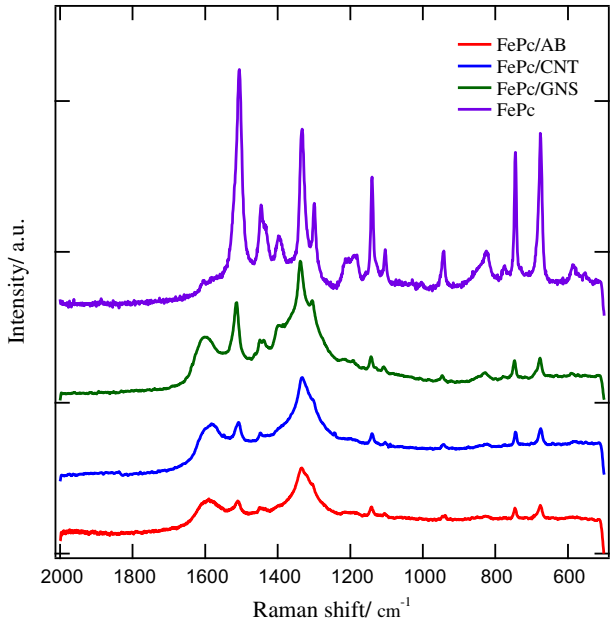

Fig. 5. Raman spectroscopy of FePc supported on various carbon materials and FePc.

and FePc/AB, respectively. Moreover, the capacity was 632.4, 865.6 and 795.4 mA h g^{-1} for FePc/CNTs, FePc/GNS and FePc/AB, respectively. This data shows that the electrochemical performance of Li–air batteries was dependent on the kinds of nanocarbon support materials. These high electrochemical performances of FePc/CNTs and FePc/GNS in comparison with the FePc/AB are considered to derive from the more efficient formation of triple-phase boundaries around dispersed FePc on the CNTs forming. The high conductivity of CNTs and GNS is also considered to contribute to the high electrochemical performance. Furthermore, we have reported that the discharge voltage of 20 wt% Pt/CB exhibited about 3.05 V in the same condition previously [7]. This means that the FePc/CNTs exhibits an excellent catalytic activity of ORR, which shows the near that of 20 wt% Pt/CB. It is thus considered that the CNTs are expected as a promising carbon substrate for electrocatalysts for Li–air battery. However, this discharge performance did not agreed with the catalytic activity of ORR, which showed the same onset potential of ORR for all samples. Although the reason why the difference of discharge performance depends on carbon substrate is not clear for FePc supported on various carbon materials, it is considered that the problems are the cathode electrode fabrication such as the efficient formation of the triple-phase boundaries of gas-electrode–electrolyte and the contact of the catalyst–electrolyte interface. This weak point is being studied further.

The cyclic performance of the cathode electrode is very important to use the Li–air battery as a secondary battery. In order to investigate the stability of FePc/carbon for Li–air battery with hybrid electrolyte, the cyclic performance for all measured samples were carried out at a current density of 0.5 mA cm^{-2} for 2 h to each charge and discharge at 30th cycle under the alkaline condition. Fig. 4(a–c) gives the cycle performance curves obtained for FePc/GNS, FePc/CNTs and FePc/AB. The cycling behavior of FePc/GNS and FePc/CNTs showed the stability after 5th cycle. In contrast, the FePc/AB showed the very stable cyclic performance. Fig. 4d shows the voltage gap between discharge and charge obtained for all measured samples to investigate the overpotential of cathode electrode. At 1st cycle, the difference voltage between discharge and charge is 0.67, 0.85 and 1.05 V for FePc/GNS, FePc/CNTs and FePc/AB, respectively. Moreover, the voltage gap between discharge and charge after 30th cycle was increased to 1.3, 1.2 and 1.25 V for FePc/GNS, FePc/CNTs and FePc/AB, respectively. It is thus indicated that the cyclic performance of all measured samples were degraded with increasing cycle numbers. Especially, the FePc/GNS showed the higher voltage gap after 30th cycle in comparison with both samples, even though the voltage gap at 1st cycle was lower than those of both samples. Meanwhile, the degree change of voltage gap between 1st and 30th cycle for FePc/CNT and FePc/AB revealed less (0.35, 0.2 V) than that of FePc/GNS (0.63 V). This showed that the FePc/CNTs and FePc/AB are much more stable under studied conditions. Previously, we have reported that the GNS with many defects or vacancies on the surface was susceptible to corrosion during charge–discharge process than that of heat-treatment due to the reconstruction of graphite surface by heat-treatment [7]. Thus, such difference in durability of cycle performance depends on the carbon materials may be attributed to the morphology and to the difference surfaces structure of carbon consisting of graphene sheet.

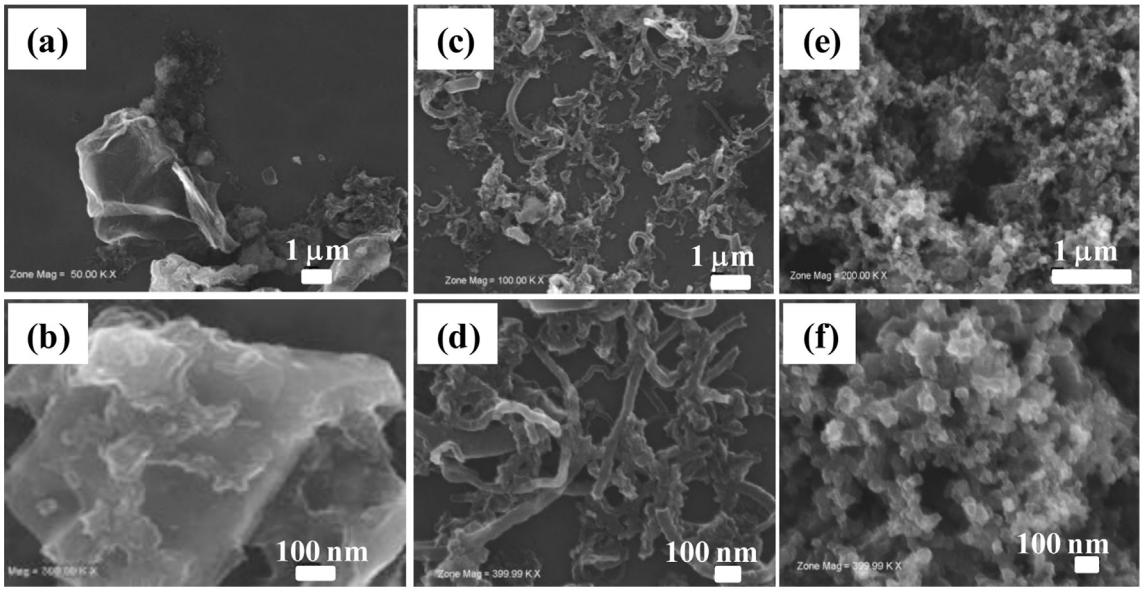

Fig. 6. SEM images of FePc/GNS (a)(b), FePc/CNTs (c)(d), and FePc/AB (e)(f).

Fig. 5 shows the Raman spectroscopy of FePc/CNTs, FePc/GNS, FePc/AB and FePc. The Raman signals attributed to FePc could be observed in the spectra of FePc/GNS, FePc/CNTs and FePc/AB. It might be considered that FePc was fixed with carbon materials such as GNS, CNTs and AB, and the electronic characteristics of carbons and FePc were not almost changed after doping. However, the Raman spectrum of FePc/GNS showed the strong intensity of peak originated from FePc comparison with FePc/CNTs and FePc/AB, indicating that the FePc was not fixed uniformly on surface of GNS. Furthermore, Raman spectra of the all measured samples also showed the G band at about 1580 cm^{-1}, which originated from the Raman-active E_{2g} mode of carbon and reflect the structure of sp^2 hybridized carbon atoms [19,20]. The G band for all FePc/carbon didn't reveal any notable change, so there is no prominent charge transfer between carbon materials and FePc. However, we didn't observe any significant difference in the Raman result for all FePc/carbon catalysts.

SEM measurements were also carried out to observe the morphology of the FePc/carbon. Fig. 6 displays the typical SEM images obtained for FePc/GNS, FePc/CNTs and FePc/AB. The SEM images showed the FePc was deposited locally and agglomerated each other on the GNS (Fig. 6(a,b)). Additionally, the CNTs also were not mixed with the FePc homogeneously. On the other hand, it was confirmed that the FePc was fixed on AB homogeneously, because we could not find the FePc in the AB.

The detailed mechanism of electrochemical performance for FePc catalysts supported on various carbon materials is not yet. However, it was found that not only the electrocatalytic activity of ORR was enhanced by combination between FePc and carbon materials, but also the electrochemical performance for Li–air battery significantly depends on the kind of carbon substrate materials. The difference may be attributed to the difference morphology and surface structure of carbon substrate materials. It is considered that the high electrochemical performance of FePc/CNTs is ascribed to the one direction morphology with the flat surface structure of CNTs, which is easy to adsorb FePc on CNTs by non-covalent π–π interactions and lead to good electro conductivity. It is thus expected that controlling the carbon substrate for catalysts leads to further enhanced catalytic activity of electrocatalysts for Li–air battery.

4. Conclusions

We prepared a composite of FePc and various carbon supports such as CNTs, GNS and AB and investigated its ORR performance and electrochemical performance of Li–air batteries with hybrid electrolyte. The electrochemical examination of the ORR shows that the FePc catalysts supported on various carbon revealed the high catalytic activity toward ORR with 4-electron pathway for oxygen reduction. However, the electrochemical performance of Li–air battery showed that the FePc/CNTs exhibited the highest discharge performance and good stability of cyclic performance comparison with both samples. It is considered that the electrochemical performance varied depending on the carbon materials used as support of FePc. The results of present work suggest the import factor leading to both high ORR activity and high electrochemical performance of Li–air is the combination between FePc and carbon materials with electrical properties and crystallographic structure.

Acknowledgments

LISICON (lithium super-ion conductor glass film) is provided by the Ohara Company in Japan.

References

[1] K.M. Abraham, Z. Jiang, J. Electrochem. Soc. 143 (1996) 1–5.
[2] T. Ogasawara, A. Débart, M. Holzapfel, P. Novák, P.G. Bruce, J. Am. Chem. Soc. 128 (2006) 1390–1393.
[3] A. Debart, A.J. Paterson, J. Bao, P.G. Bruce, Angew. Chem., Int. Ed. 47 (2008) 4521–4524.
[4] A. Armand, J.M. Tarascon, Nature 451 (2008) 652–657.
[5] T. Zhang, N. Imanishi, S. Hasegawa, A. Hirano, J. Xie, Y. Takeda, O. Yamamoto, N. Sammes, J. Electrochem. Soc. 155 (2008) A965–A969.
[6] Y. Wang, H. Zhou, J. Power Sources 195 (2010) 358–361.
[7] E. Yoo, H. Zhou, ACS Nano 5 (2011) 3020–3026.
[8] T. Zhang, N. Imanish, Y. Shimonish, A. Hirano, Y. Takeda, O. Yamamoto, N. Sammes, Chem. Commun. 46 (2010) 1661–1663.
[9] Z. Chen, D. Higgins, A. Yu, L. Zhang, J. Zhang, Energy Environ. Sci. 4 (2011) 3167–3192.
[10] J. Zagal, M. Paez, A.A. Tanaka, J.R. Dossantos, C.A. Linkous, J. Electroanal. Chem. 339 (1992) 13–30.
[11] R. Chen, H. Li, D. Chu, G. Wang, J. Phys. Chem. C 113 (2009) 20689–20697.
[12] G. Dong, M. Huang, L. Guan, Phys. Chem. Chem. Phys. 14 (2012) 2257–2259.
[13] W.S. Hummers, R. Offeman, J. Am. Chem. Soc. 80 (1958) 1339.
[14] S. Wang, D. Yu, L. Dai, J. Am. Chem. Soc. 133 (2011) 5182–5185.
[15] J. Wu, H. Yang, Nano Res. 4 (2011) 72–82.
[16] E. Yeager, J. Mol. Catal. 38 (1986) 5–25.
[17] N.M. Markovic, P.N. Ross, Surf. Sci. Rep. 45 (2002) 117–229.
[18] K.S. Yang, G. Mul, J.A. Moulijn, Electrochim. Acta 52 (2007) 6304–6309.
[19] R.V. Hull, L. Li, Y.C. Xing, C.C. Chusuei, Chem. Mater. 18 (2006) 1780–1788.
[20] H. Tong, H.L. Li, X.G. Zhang, Carbon 45 (2007) 2424–2432.